

# Spatial Control of Spontaneous Fluorescence by Stimulated Emission

Kathrin Spendier  
Advisor: Dr. James L. Thomas

Undergraduate Honors Research Thesis  
University of New Mexico Physics and Astronomy Department  
November 22, 2006

## Abstract

The objective of this project was to determine whether an evanescent wave excited by a low power red Helium Neon laser (HeNe) (wavelength of 632 nm) could reduce spontaneous singlet emission in a fluorescent dye. We found that it could not. Instead, the spontaneous emission increased. We attributed this result to stimulated emission from molecules in the triplet state, which depopulates the triplet state and thus increases the populations of ground state and singlet state molecules. We carried out a series of experiments to test our hypothesis. We confirmed an increase in spontaneous fluorescence of  $0.021 \pm 0.011$  %, substantially less than a theoretical value of 1.29%. Uncertainties in beam profile and in stimulated emission cross-sections (especially from the triplet state) may account for the discrepancy.

## Table of Contents

1	Introduction.....	3
2	Theory.....	4
	2.1.1 Total Internal Reflection.....	4
	2.1.2 Evanescent Waves.....	5
	2.2 Fluorescence.....	6
	2.2.1 Fluorescence at Steady State.....	7
	2.2.2 Stimulated Emission at Steady State.....	8
	2.3 The Stokes Shift.....	9
3	Experiments.....	10
	3.1 Dye Selection.....	10
	3.2 Dye Preparation.....	10
	3.3 Apparatus.....	10
	3.4 Experiment 1.....	11
	3.4.1 Data collected.....	12
	3.4.2 Conclusion.....	13
	3.5 Experiment 2.....	14
	3.5.1 Data Collected.....	15
	3.5.2 Conclusion.....	15
	3.6 Experiment 3.....	16
	3.6.1 Data Collected.....	17
	3.6.2 Results and Conclusion.....	18
4	Discussion.....	21
5	Conclusion.....	22
6	Acknowledgements.....	23
7	References.....	23
8	Appendix.....	25
	8.1 Calculation of Surface Plasmon Resonance.....	25
	8.1.1 SPR Matlab Files.....	29
	8.2 Estimated Magnitude of Fluorescence Depletion in the Absence of Triplet State Effects.....	32

8.3	Tabulated Raw Data.....	33
8.3.1	Experiment 1.....	33
8.3.2	Experiment 2.....	35
8.3.3	Experiment 3.....	36
8.4	Appended Figures.....	39

## 1. Introduction

Fluorescence is the radiation emitted from an atom or a molecule (fluorophore) following the relaxation of an electron from an excited state to the ground state. If a fluorophore absorbs a photon with an energy matching the difference between the ground state and an excited state, it can reemit a photon by returning the electron to the ground state. In liquids, vibrational relaxation of the excited state causes the emission to be at longer wavelength than the excitation (the Stokes Shift). The detection of this lower energy photon confirms fluorescence. For a collection of randomly oriented fluorophores, and in the absence of an electromagnetic field matched to the emission energy, the fluorescent photons are emitted isotropically. This is called spontaneous emission.

Excited molecules may instead undergo stimulated emission if an electromagnetic field of suitable frequency is present. In this case, the emitted photon adds coherently to the stimulating field. It has recently been demonstrated [1] [3] that the stimulating field does not have to be a free-space propagating wave – waves that are confined to interfaces, such as evanescent waves, can also cause stimulated emission. The stimulated emission can be observed as an enhanced internal reflection (greater than “total”) for the probe beam. Evanescent waves decay exponentially with distance from the interface, with a typical decay length much shorter than  $\lambda$  (wavelength of the excitation beam). Thus, both fluorescence excitation and stimulated emission processes can be confined to a very thin (100 nm) zone near the interface. Evanescent wave excitation has long been used to image fluorescent biological specimens with improved resolution (perpendicular to the interface).

One of the most exciting current applications of stimulated emission is to trim the spatial distribution of excited fluorophores [2] for enhanced resolution in fluorescence microscopy. The stimulated emission is “discarded” (not detected); the fluorophores that can then undergo spontaneous emission must be in a region that was excited by the pump beam, but not by the probe beam. This excluded region can be much smaller than the classical diffraction limit. In the case of evanescent illumination, it may be possible to use an exciting wave with a gentler decay (by changing the angle of incidence), and a stimulated emission wave with a sharp decay to deplete spontaneous fluorescent very near the surface. The detected spontaneous emission would then arise from a ‘section’ of the sample above the interface. It may also be possible to use the enhanced electromagnetic fields associated with surface plasmons (and in particular plasmons

excited in metallic nanoislands) to ‘trim’ the distribution of spontaneous fluorescence so as to improve spatial (lateral) resolution in imaging. .

Although stimulated emission into confined (evanescent) waves has been observed, the depletion of spontaneous emission has not yet been reported. This depletion effect is important if confined waves are to be used for stimulated emission fluorescence microscopy.

## 2. Theory

### 2.1.1 Total Internal Reflection

Light bends away from the normal when it is incident on a lower index medium from a higher index medium. At a particular incident angle, the angle of refraction will be  $90^\circ$ , and the refracted ray will just skim the surface (Figure 1). The incident angle at which this occurs is called the critical angle ( $\theta_c$ ). Using Snell’s law,

$$n_1 \sin(\theta_i) = n_2 \sin(\theta_t) \quad \text{Eq.1}$$

where  $\theta_{i(t)}$  is the incident (transmitted) angle and  $n_{1(2)}$  is the refractive index. The critical angle,  $\theta_c$ , is the angle of incidence when  $\theta_t = 90^\circ$ . Thus,

$$\sin(\theta_c) = \frac{n_t}{n_i} \quad \text{Eq.2}$$

for  $\theta_i > \theta_c$ . The absence of a transmitted wave is referred to as total internal reflection (TIR).

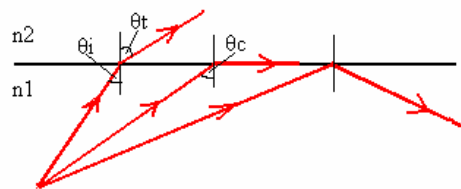


Figure 1: Total internal reflection of light

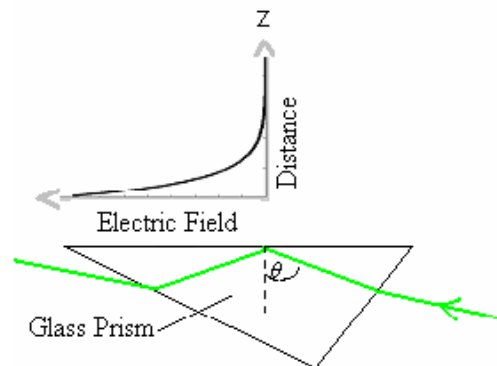


Figure 2: Total internal reflection using Kretschmann configuration [14]. The electric field vector exponentially decays with distance from the interface.

### 2.1.2 Evanescent Waves

Evanescent waves are based on the phenomena of total internal reflection (TIR). Although the fully reflected beam does not lose any net energy across the TIR interface, the light beam leaks an electrical field intensity called an evanescent wave into the low refractive index medium. The amplitude of this field wave decreases exponentially with distance from the surface (Figure 2).

According to Snell's law, total internal reflection occurs when,  $\theta_c < \theta_i$ . Beyond the critical angle, the angle  $\theta_t$  formally becomes imaginary (Figure 1). To understand how the angle becomes imaginary and the physical significance of the imaginary angle, we use Snell's law and the following equation:

$$\cos(\theta_t) = \sqrt{1 - \sin^2(\theta_t)} \quad \text{Eq.3}$$

Snell's law can be used to rewrite this identity:

$$\cos(\theta_t) = \sqrt{1 - \left(\frac{n_i}{n_t}\right)^2 \sin^2(\theta_i)} = \sqrt{1 - \left(\frac{\sin(\theta_i)}{\sin(\theta_c)}\right)^2} \quad \text{Eq.4}$$

Over the interval  $0 > \theta > \pi/2$ , we have  $0 > \sin(\theta) > 1$  so that  $\sin(\theta_i)/\sin(\theta_t) > 1$  when  $\theta_c < \theta_i$ . This leads to the conclusion that  $\cos \theta_t$  is imaginary:

$$\cos(\theta_t) = i \sqrt{\left(\frac{\sin(\theta_i)}{\sin(\theta_c)}\right)^2 - 1} = -i\alpha \quad \text{Eq.5}$$

where

$$\alpha = -\sqrt{\left(\frac{\sin \theta_i}{\sin \theta_c}\right)^2 - 1}$$

If an incoming electromagnetic wave hits an interface such as in Figure 3, where the plane of incidence is the x-y plane, one can describe the transmitted wave as follows [4]:

$$\tilde{E}_t(\vec{r}, t) = \tilde{E}_{0t} e^{-i(\vec{k} \cdot \vec{r} - \omega t)} \quad \text{Eq.6}$$

$$\vec{k}_t = k_t (\sin(\theta_t) \hat{x} + \cos(\theta_t) \hat{z}) \quad \text{Eq.7}$$

Substituting  $-i\alpha = \cos(\theta_t)$  (Eq.5) and  $\sin^2(\theta_t) = 1 + \alpha^2$  (Eq.3), one obtains:

$$\tilde{E}_t(\vec{r}, t) = \tilde{E}_{0t} e^{-\alpha k_r z} e^{-i(k_x x \sqrt{1+\alpha^2} - \omega t)} \quad \text{Eq.8}$$

The transmitted wave propagates parallel to the surface, along the x axis, and is attenuated exponentially in the z direction, normal to the propagation direction. This is called an evanescent wave.

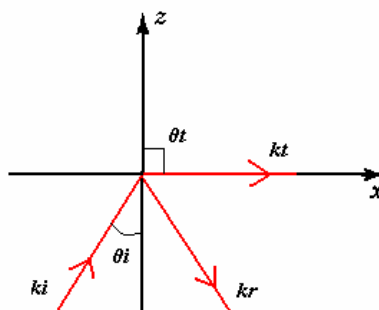


Figure 3: Geometry that establishes the conventions for the optics at an interface.

## 2.2 Fluorescence

Light can excite a molecule from the ground state ( $S_0$ ) (Figure 4) [5] into a higher energy state ( $S_1$ ). From this state there exist two important pathways for relaxation back to the ground state: fluorescence and phosphorescence. For both pathways, the first step is internal conversion, in which the excited molecule thermalizes by exchanging vibrational quanta with its environment. (In addition, in a polar solvent, the solvent molecules will reorient around the excited state dipole.) These processes are fast; within less than a nanosecond, the molecule has reached one of the lowest vibronic sublevels of the first electronic excited state.

After thermalization, the molecule may emit a photon to return to the electronic ground state (FL). This emission is fluorescence. During this relaxation fluorescence (FL) may occur. Typically, after absorption of a photon (ABS) the molecule reaches thermal equilibrium with its surroundings in much less than a nanosecond. For fluorescent molecules, the decay via photon emission from  $S_1$  to  $S_0$  takes a few nanoseconds [5]. The decay is relatively fast (compared with phosphorescence, see below) because the excited electron can decay back to the ground state without violating the Pauli exclusion principle. While in the excited state, however, interactions with the environment may result in a spin flip (intersystem crossing, ISC). The molecule is now said to be in a “triplet state” ( $T_1$ ), and direct decay to the ground state is forbidden. The molecule eventually decays to the ground state through concerted photon emission and

environmental interactions. Emission from the triplet state is termed phosphorescence (PH). Phosphorescence lifetimes are typically microseconds to seconds.

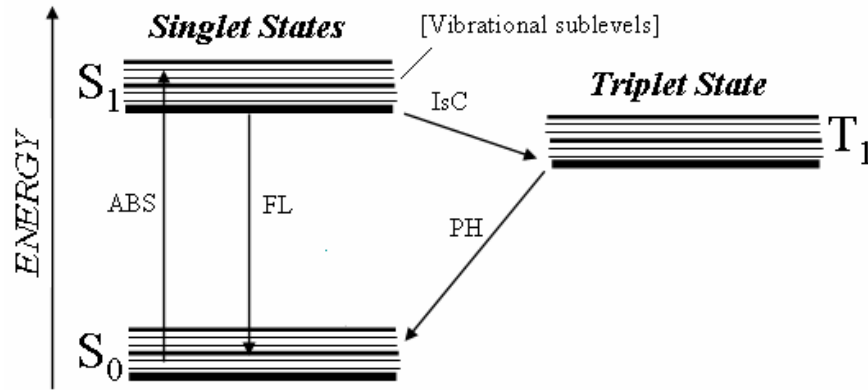


Figure 4: Atomic energy level diagram

### 2.2.1 Fluorescence at Steady State

We can write a set of conceptual rate equations (see, for example, [15]) to describe the populations of molecules in the singlet, triplet, and ground states. These equations relate the interplay among the absorption, spontaneous emission, stimulated emission and intersystem crossing at steady state. These equations are as follows:

$$\frac{dn_g}{dt} = -\sigma_a I_g n_g + \frac{n_t}{\tau_t} + \frac{n_s(1-\alpha)}{\tau_s} = 0 \quad \text{Eq.9}$$

$$\frac{dn_s}{dt} = \sigma_a I_g n_g - \frac{n_s(1-\alpha)}{\tau_s} - \alpha \frac{n_s}{\tau_s} = 0 \quad \text{Eq.10}$$

$$\frac{dn_t}{dt} = \alpha \frac{n_s}{\tau_s} - \frac{n_t}{\tau_t} = 0 \quad \text{Eq.11}$$

where:

$n_s$  = fraction of molecules in 1<sup>st</sup> excited state (singlet state)

$n_t$  = fraction of molecules in triplet state

$n_g$  = fraction of molecules in ground state

$\tau_t$  = triplet state lifetime

$\tau_s$  = singlet state lifetime

$I_g$  = intensity of pump beam (in photons per unit area per unit time)

$I_r$  = intensity of probe beam (in photons per unit area per unit time)

$\sigma_a$  = absorption cross-section

$\sigma_s$  = stimulated emission cross-section

$\alpha$  = quantum yield of intersystem crossing

Equations 9, 10, and 11 describe the number of molecules in the ground state, first excited state, and triplet state at steady state. The terms in equation 9 describe excitation,

phosphorescence, and fluorescence respectively. The number of molecules in the ground state decreases via absorption and intersystem crossing, whereas fluorescence and phosphorescence populate the ground state. The first term in equation 10 describes the number of molecules in the first excited singlet state due to absorption. Fluorescence and intersystem crossing depopulate this state. Finally, intersystem crossing populates the triplet state, which is depopulated by phosphorescence (Eq.11).

### 2.2.2 Stimulated Emission at Steady State

As mentioned earlier, if a molecule lies in the first excited state it can drop to the ground state by emitting a photon. Since this transition occurs spontaneously, it is called spontaneous emission. (Figure 5). Alternatively, while in the excited state, the molecule can be illuminated with an incoming photon, which has exactly the same energy as the transition that would spontaneously occur. The atom may be stimulated by the incoming photon to return to the ground state and simultaneously emit a photon at that same transition energy. A single photon interacting with an excited atom can therefore result in amplification. If the emitted photons are viewed as a wave, the stimulated emission will oscillate at the incoming light's frequency and be in phase resulting in amplification of the original light wave's intensity (Figure 6).

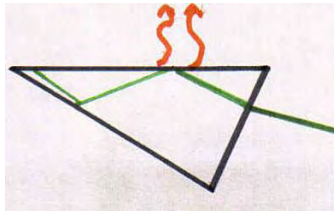


Figure 5: Fluorescence

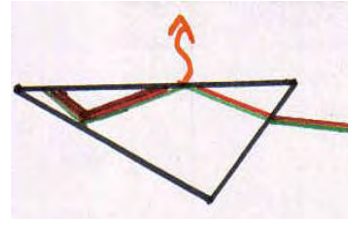


Figure 6: Depleted fluorescence

One can describe stimulated emission by these three equations:

$$\frac{dn_s}{dt} = \sigma_a I_g n_g - \frac{n_s(1-\alpha)}{\tau_s} - \sigma_s I_r n_s - \alpha \frac{n_s}{\tau_s} = 0 \quad \text{Eq.12}$$

$$\frac{dn_t}{dt} = \alpha \frac{n_s}{\tau_s} - \frac{n_t}{\tau_t} - \sigma_s I_r n_t = 0 \quad \text{Eq.13}$$

$$n_g + n_s + n_t = 1 \quad \text{Eq.14}$$

Equation 12 (Eq.12) and 13 (Eq.13) differ from equation 9 (Eq.9) and 11 (Eq.11) only by the stimulated emission term. The third term in equations 12 and 13 describe the stimulated depletion of the first excited state and the triplet state respectively. The stimulated emission cross-section of the triplet state ( $\sigma_t$ ) has not been measured, as so was assumed to be the same as the stimulated emission cross-section of the singlet state ( $\sigma_s$ , Eq.13). (This may be a major source of the discrepancy between the calculations and the observations, see below.) In order to insure normalization of the total number of molecules, the fraction of molecules in the ground state, first excited state, and triplet state have to add up to one (Eq.14). These equations can be combined to get the number of molecules in the ground state ( $dn_g/dt$ ). With this system of equations one can solve for the number of molecules in each state, assuming the other parameters are known.

### 2.3 The Stokes Shift

At low temperatures, the absorption of a photon generally occurs from the lowest vibronic ground state level to one of the excited state vibronic levels. After relaxation, the emission occurs from the lowest excited state vibronic level to one of the higher vibronic levels of the ground state manifold. Consequently, the fluorescence occurs at lower energies than the absorption and thus is red-shifted. This phenomenon of fluorescence being red-shifted from the absorption is called the Stokes shift. [Note: laser cooling is possible only because a photon can be absorbed from a vibrationally excited electronic ground state, resulting in an anti-Stokes effect.]. Quantitatively the Stokes shift is the difference between the peak wavelengths in the absorbance and the emission spectra. In Figure 7 we show the absorption and emission spectra of fluorescein as an example [6]. (I used Rhodamine B, not fluorescein in the experiments presented here.)

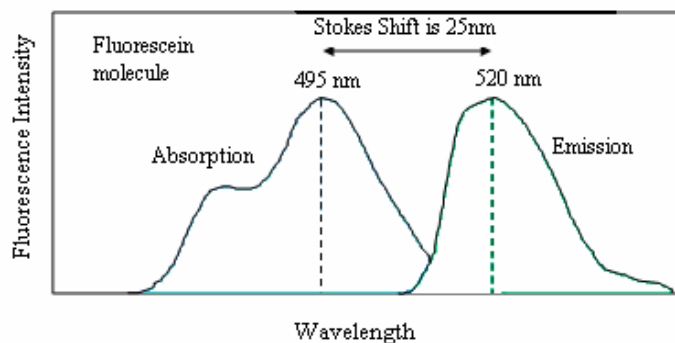


Figure 7: Absorption and emission spectrum of a fluorescein molecule.

### 3. Experiments

#### 3.1 Dye Selection

The green HeNe should pump the fluorescent molecules into the first excited state, whereas red light illumination acts as ‘probe’. Hence, the fluorophore for this series of experiments was chosen to be so that it can be excited at 543 nm with a green HeNe laser and has a detectable emission at 632 nm. Moreover, the selected dye should not absorb a photon at a wavelength of 632 nm. At this wavelength, the red probe beam should cause the dye to emit its photon into the evanescent field and thus decrease the observed spontaneous fluorescence. Absorption at 632 nm would counteract this effect. Rhodamine B (RhB) fulfills these requirements, as may be discerned from the absorption and emission spectra shown in Figures A4 and A5.

#### 3.2 Dye Preparation

Rhodamine B is a well-known fluorescent dye that can be dissolved in water and ethanol. Since the quantum yield, which defines the efficiency of the fluorescence process, for RhB dissolved in ethanol is higher than in water, ethanol was used as solvent. The fluorescence signal does not only depend on the quantum yield, but also on the dye concentration. After testing different concentrations of RhB in ethanol, we found that 70 mM produced the largest fluorescence signal. (High dye concentrations lead to decreases in fluorescence, caused by dye-dye interactions. This is known as ‘self-quenching’.) This concentration of 70 mM was used throughout the experiment. In order to align the red beam, I used a fluorophore called Oxadiazocyanine or Cy5. that was excitable by 632 nm light. Cy5 was dissolved in water. The fluorescence emission from this dye allowed me to align the red laser to superimpose the red evanescent spot on the green.

#### 3.3 Apparatus

We used a home built microscope (Figure 8a) to detect fluorescence. The microscope consists of a 16 cm long aluminum tube holding a microscope objective (10X). Inside the tube, two Raman edge filters (RF) cut out light with wavelength below 633 nm. These filters are needed to separate the emitted spontaneous fluorescence from the much brighter red probe beam. Three translation stages position the tube in the x, y, and z directions. The detector was mounted on top of the microscope.

We used a BK7 right angle prism (Edmund Optics) to produce evanescent waves. The prism was mounted with a specially designed holder (Figure 8b), which is adjustable in the vertical direction. The sample was placed underneath a cover slip on top of the prism. To prevent evaporation of the fluorescence dye, the cover slip was sealed with nail polish. (Traces of acetone solvent do not affect dye fluorescence [16]).

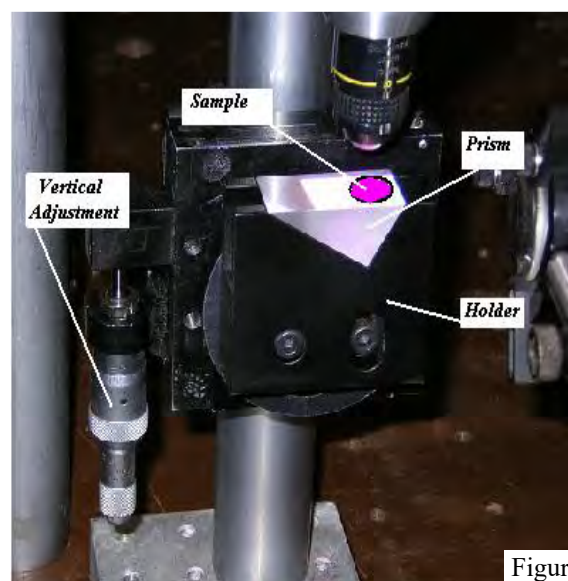
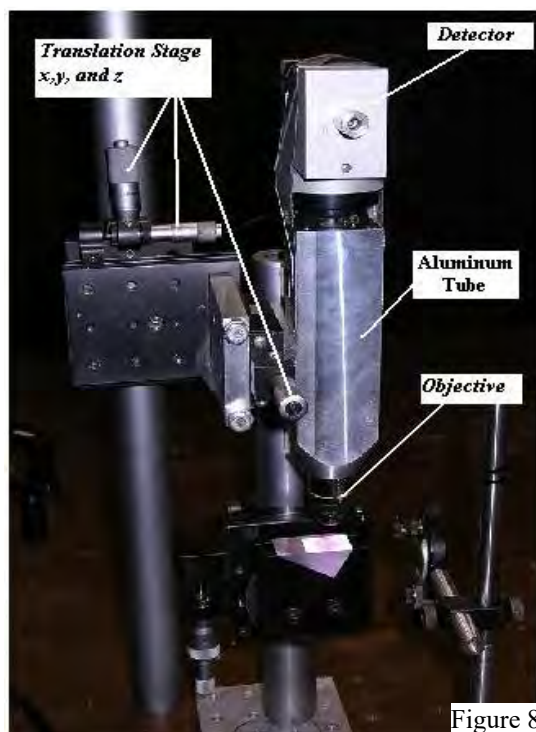


Figure 8a and 8b: Experimental apparatus

### 3.4 Experiment 1

This research is broken down into three separate experiments, which will be described in detail below. The experimental goal was to measure the variation in the fluorescence signal due to red light illumination. The experimental setup for the fluorescence measurement is depicted in Figure 9. We estimated the fluorescence depletion (ignoring triplet state effects) to be one part in 1000 (refer to appendix, 8.2). We used lock-in detection to measure this small signal compared to the fluorescence background. The probe beam signal was mechanically chopped at 270 Hz. An avalanche photodiode (APD) detected the fluorescence signal. Finally, we analyzed the preamplified signal from the APD output with a lock-in amplifier. The signal from the optical chopper (CH) and the photo diode (PD) were used as references for the lock-in amplifier.

In order to measure the change in spontaneous emission caused by the probe beam, the green pump and red probe beam have to illuminate the sample at the same location. This was achieved by adjusting the position of the detector relative to the probe beam. Oxadiazocyanine, Cy5 was used for detector alignment purposes. Cy5 is excited by the probe beam (Figure A6), and emits at higher wavelength than the Raman edge filter (RF) cut off. After positioning the detector to maximize the signal from the Cy5 solution, we aligned the pump beam with the dichroic filter (DF) using RhB dissolved in ethanol. For this alignment we used and positioned CH between mirror one (M1) and DF. The probe beam was successfully aligned when we detected the maximal fluorescence signal from RhB.

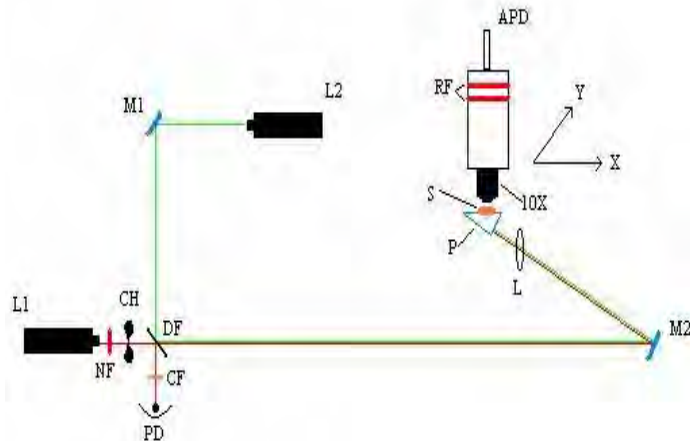


Figure 9: Experimental setup of experiment 1.

Equipment depicted in Figure 9:

- L1: probe beam (red 632.8nm) JDS Uniphase, Model 1652
- L2: pump beam (green 543nm) Uniphase, Model 1507P
- NF: notch filter for He-Ne 632.8nm
- CH: optical chopper at 270 Hz (Thorlabs, Model MC 100)
- DF: dichroic filter at 45°
- CF: color filter (orange)
- PD: photo diode (Thorlabs, Model PDA55)
- M1: mirror 1
- M2: mirror 2
- P: glass prism (BK7), Edmund Optics
- S: sample (Oxadiazocyanine (Cy5)-dissolved in water, Rhodamine B (RhB)-dissolved in ethanol)
- 10X: 10X objective, NA 0.24
- L: biconvex lens, focal point 5cm
- RF: two Raman edge filters (633nm)
- APD: photo multiplier tube (Hamamatsu, Model C5460)

Needed equipment not included in Figure 9:

- Digital oscilloscope, Instek, Model GDS-820
- Low noise preamplifier, Signal Recovery, Model 5113
- Lock-in amplifier, Princeton Applied
- Research, Model 5101, Power supply R.S.R., Model PW-3032

### 3.4.1 Data Collected:

The chopper operated at a frequency of 270 Hz. The applied voltage to the APD was 23.7 V and the APD output was pre-amplified by a factor of 50. The measured power of the green pump beam and red probe beam was 120  $\mu$ W and 250  $\mu$ W respectively. Since the time constant of the lock-in amplifier was set to its maximum of 30 s, data was taken every 40 s during a period of 200 seconds. The raw data is tabulated in Tables A1 and A2. The final data, after an averaging process, is depicted in Table 1. The

uncertainties in the measured fluorescence change were calculated with the standard error of the mean.

Table 1:

#	Green Pump Beam	Red Probe Beam	Reference Signal for Lock-In Input	Measured Amplitude of Fluorescence Modulation	Notes
1	chopped	off	chopped	$100 \pm 2.5$ mV	
2	on	chopped	PD	$48.5 \pm 0.99$ $\mu$ V	Signal in phase with probe beam
3	off	chopped	PD	$27.5 \pm 0.22$ $\mu$ V	

### 3.4.2 Conclusion

We expected to see fluorescence depletion from the singlet state if RhB was excited continuously with the pump beam and chopped by the probe beam. From Figure 10, one can see that the depletion effect should be in phase with the chopped probe beam, and manifest itself by decreasing the spontaneous emission. If we compare measurements 2 and 3 in Table 1, we see that the fluorescence signal instead increased when the red probe beam was present. After subtracting the signal amplitude of measurement 3 from measurement 2, the calculated fluorescence increase due to red light illumination is  $0.021 \pm 0.002$  %.

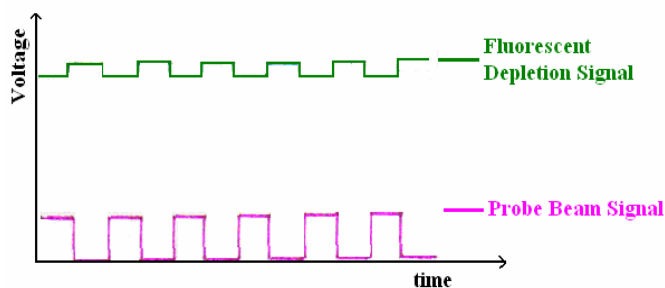


Figure 10: Fluorescence depletion signal is in phase with red light illumination.

We developed two possible reasons why the signal was bigger with the red probe beam chopped and green pump beam on than with the probe beam chopped alone. These hypotheses are:

#### *Hypothesis 1*

The absorption of the red probe beam by molecules in the triplet state could excite molecules into a second excited triplet state, which could then relax via photon emission from this state.

### Hypothesis 2

The probe beam causes stimulated emission not only from the excited singlet state, *but also from the triplet state*. This depletes the triplet state, which decreases the lifetime of the molecules in this state. This effect results in an increase of the number of molecules in the ground state. Hence, we are pumping more molecules into the first excited state, which increases the fluorescence.

### 3.5 Experiment 2

A second experiment was conducted to test the two hypotheses stated above. The premise is this: if the triplet state can absorb red light, then the transmitted intensity of red light through a dye sample should *decrease* if we also illuminate with a green beam. (The green beam will pump the majority of the excited state molecules into the triplet state. Because the triplet lifetime is very long,  $6.0 \mu\text{s}$  [7], even with a low intersystem crossing probability (0.6%), under steady illumination the population of triplet state molecules is 3.6 times higher than the population of singlets.)

The experimental setup is shown in Fig. 11. A chopped (270 Hz) green beam and a steady red beam were passed through a cuvette containing a dye solution. There is a small crossing angle, to maximize the overlap of the two beams while minimizing the amount of green light that hits the detector. Of course, a 632.8 nm narrow pass filter is also used to block the green beam. A lens (L1) was used to focus both beams, thereby increasing the fluorescence intensity and thus the fraction of dye molecules in the excited state.

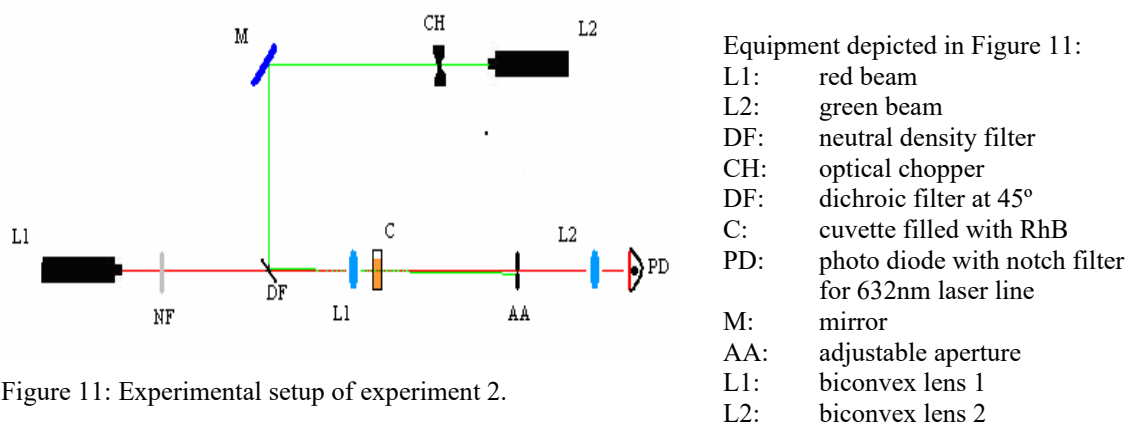


Figure 11: Experimental setup of experiment 2.

### 3.5.1 Data Collected

Experimental Details: The concentration of RhB dissolved in ethanol in cuvette C was about 0.01 mM. The power of the red and green laser beams were 250  $\mu\text{W}$  and 120  $\mu\text{W}$  respectively. The chopper provided a reference signal for a lock-in amplifier, and the lock-in phase was adjusted so that a positive amplitude corresponded to *more red light* when the green beam was on.

Even with a good 632.8 nm notch filter, there is some small signal from the green beam alone. This was measured by blocking the red laser, and the result is shown in Table 2, line 2:  $1.54 \pm 0.02 \mu\text{V}$ . The raw data for this experiment is tabulated in Tables A3, A4, and A5.

Table 2

#	Red Probe Beam	Signal Amplitude *
1	on	$3.38 \pm 0.06 \mu\text{V}$
2	off	$1.54 \pm 0.02 \mu\text{V}$

\* This is the amplitude of the signal in phase with the chopped green beam, for red beam on and off.

### 3.5.2 Results and Conclusion

With the red probe beam on, the lock-in detects the variation in red intensity as the green beam is chopped on and off. If significant triplet state absorption occurs, then the transmitted red intensity should *fall* when the green beam is on. Instead, I observed a signal of  $3.38 \pm 0.06 \mu\text{V}$ , which is significantly larger than the ‘background’ leakage from the green beam alone. The red beam is actually getting stronger when the green beam is on. This shows that stimulated emission is occurring in this dye sample.

Because some of the molecules are in the singlet state, it is *possible* that *all* the stimulated emission comes from the singlet state, while the absorption of the triplet state is so weak that the red beam still increases in intensity on passing through the (green-) pumped sample. However, because *most* of the excited molecules are in the triplet state, the triplet state absorption would have to be very small indeed for this scenario to hold. Simply because the signal is positive, we can rigorously state the absorption cross-section in the triplet state must be less than 1/6 of the stimulated emission cross-section from the singlet.

To more precisely separate the singlet and triplet behavior, it is possible to modulate the pump at a high frequency (e.g. 40 MHz as in experiment 3.) Pumping at this frequency, the singlet state population will modulate at 40 MHz, but the triplet population will be steady (owing to the long lifetime.) Because of time constraints, I was not able to make this measurement using a 40 MHz modulation.

If the red beam causes stimulated emission *only from the singlet state*, then this beam will cause a decrease in the population of singlets, and a concomitant increase in the population of ground and triplet state molecules. If those triplets absorb the red light, this would lead to a non-linear dependence of the red signal on red beam intensity; the curve would deviate downward. I looked for such a nonlinearity by changing the red beam intensity with neutral density filters (DF), Figure 12. Over the range of accessible intensities, no evidence for non-linearity was found, supporting the hypothesis that triplets do not absorb red light.

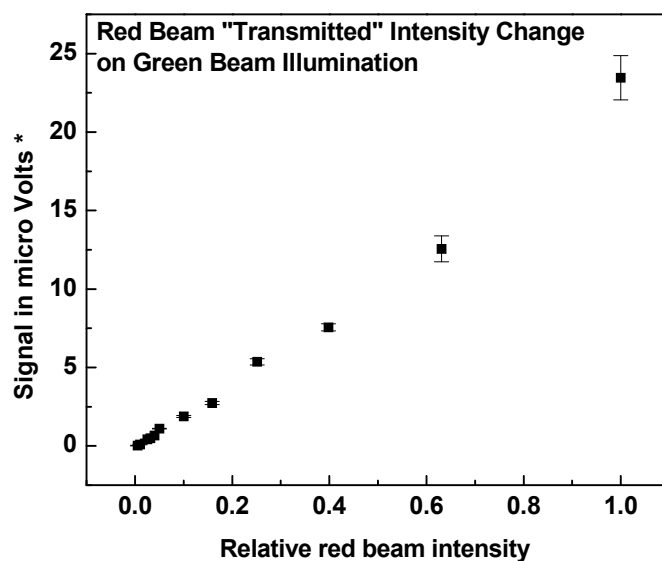


Figure 12: \*Contribution of green beam excitation (measurement #2 in Table 1) was subtracted from the measured signal amplitude. Raw data is tabulated in Table A6.

### 3.6 Experiment 3

The third and final experiment determines the fluorescence increase due to stimulated emission from the triplet state in absence of phosphorescence. As mentioned earlier (2.2), phosphorescence is the photon emission caused by a molecule in the triplet state when returning to the ground state. In experiment 1, we chopped the green pump beam at a frequency of 270 Hz. This period of 3.6 ms is long compared to the triplet state

lifetime of 6  $\mu\text{s}$ . Hence, in experiment 1 we compared signals which have different numbers of molecules in the triplet state. Since intersystem crossing cannot be stopped, we improved the experimental technique and modulated the triplet state such that the number of molecules in the triplet state did not vary over time.

In this experimental setup, as depicted in Figure 13, an acousto-optic modulator was used to modulate the green pump beam at 40 MHz. This modulation is fast compared to the triplet state lifetime of 6  $\mu\text{s}$ . An acousto-optic modulator acts like a beam splitter. It splits the incoming beam into two beams, one of which is frequency shifted. The two beams were recombined using an interferometer, which produced beats at 40 MHz.

An RF lock-in amplifier (fast) measured the corresponding modulation of the green pump beam as detected by a photo multiplier tube (PMT). Similarly, as in experiment one, the probe beam was mechanically chopped at 100 Hz to discriminate between the depletion signal and the fluorescence background. This additional modulation was detected with a second lock in amplifier (slow), whose output signal directly reflects the variation in the fluorescence signal due to depletion of triplet state population.

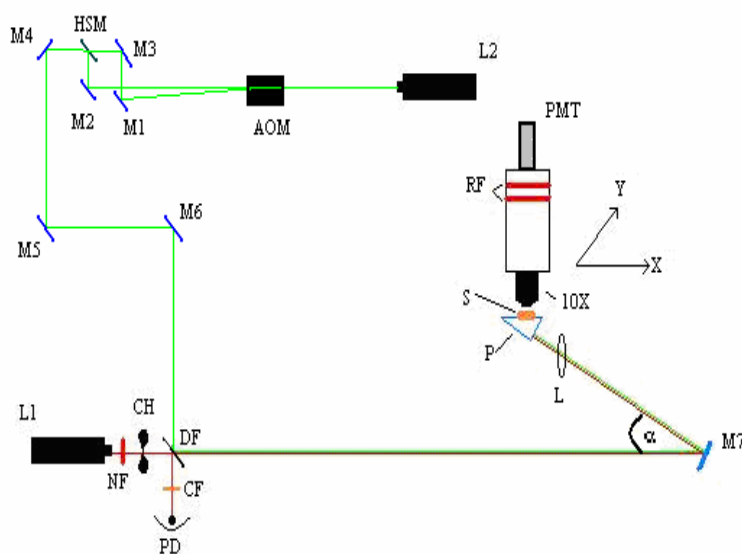


Figure 13: Experimental setup of experiment 3.

Additional equipment compared to experiment 1

- HSM: half silvered mirror
- AOM: Acousto-optic modulator, Intraction 406N
- PMT: Photo Multiplier Tube, Hamamatsu, R4220
- 10X: objective, S-Plan 10X, NA=0.3, Olympus 136228

Needed equipment not included in Figure 13:

- Digital oscilloscope, Tektronix, Model TDS 1012
- Lock-in amplifier, Princeton Applied Research, Model 5101
- RF lock-in amplifier, Stanford Research Systems, Model SR 844
- High voltage power supply, Stanford Research Systems, Model PS 325
- Frequency Synthesizer, Intraction, Model DFE dual channel

### 3.6.1 Data Collected

After alignment, we measured the fluorescence depletion by modulating the green pump beam at 40 MHz and chopped the red probe beam at 100 Hz. The time constant for the

fast lock-in amplifier was set to 300  $\mu$ s to allow the detection of the slow modulation at 100 Hz. (A longer integration time would result in effectively low-pass filtering the output of the first lock-in, attenuating the signal at 100 Hz. This was checked experimentally.) The fluorescence change was detected by a PMT, which was supplied with -1000 V (PMT gain depends on supplied voltage). To ensure that the signal measured was in phase with the probe beam, we detected the frequency of the probe beam (PD) and used this signal as reference for the slow lock in. The power of the probe beam and pump beam were 380  $\mu$ W and 40  $\mu$ W respectively. Although the time constant of the slow lock-in amplifier was set to its maximum of 30 s, the detected fluorescence signal varied significantly over time. To improve averaging, 99 measurements were collected at 5 s intervals. The results are depicted in Table 3. The uncertainties in the measured change in fluorescence signal were calculated with the standard error of the mean from the raw data tabulated in Table A7. The calculated fluorescence increase due to red light illumination is  $0.021 \pm 0.011$  %. The uncertainty was obtained through error propagation.

Table 3

#	Green Pump Beam	Red Probe Beam	Reference Signal for Lock-In Input	Measured Amplitude of Fluorescence Modulation	Notes
1	chopped	off	chopper	$218 \pm 6.25$ mV	
2	on	chopped	PD	$46.5 \pm 22.65$ $\mu$ V	Signal in phase with probe beam

### 3.6.2 Conclusion

This experiment showed that red beam illumination causes stimulated emission from the triplet state. The red probe beam cannot directly contribute to the 40 MHz fluorescence signal, since the red probe beam itself is modulated at a frequency of 100 Hz. In order to compare our result to theory, we used the rate equations of stimulated emission at steady state (Eq.12, Eq.13, and Eq.14). After solving the rate equations describing stimulated emission for the number of molecules in the singlet ( $n_s$ ) and triplet ( $n_t$ ) state, the known parameters were used to extract theory curves. The numbers of molecules in the first excited state and triplet state are described as follows:

$$n_s = \frac{(1 + \sigma_s I_r \tau_t) \sigma_a I_g \tau_s}{\sigma_a I_g \alpha \tau_t + \sigma_a I_g \tau_s + \sigma_a I_g \tau_s \sigma_s I_r \tau_t + 1 + \sigma_s I_r \tau_t + \sigma_s I_r \tau_s + \sigma_s^2 I_r^2 \tau_s \tau_t} \quad \text{Eq. 15}$$

$$n_t = \frac{\sigma_a I_g \alpha \tau_t}{\sigma_a I_g \alpha \tau_t + \sigma_a I_g \tau_s + \sigma_a I_g \tau_s \sigma_s I_r \tau_t + 1 + \sigma_s I_r \tau_t + \sigma_s I_r \tau_s + \sigma_s^2 I_r^2 \tau_s \tau_t} \quad \text{Eq. 16}$$

From literature and previous power measurements, we obtained the values of the following parameters:

$\tau_t$  = triplet state lifetime = 6.0  $\mu$ s [7]

$\tau_s$  = singlet state lifetime = 10 ns [5]

$I_r$  = intensity of red probe beam\* =  $6.9 \times 10^{21}$  photons/m<sup>2</sup>sec

$I_g$  = intensity of green probe beam\* =  $1.9 \times 10^{21}$  photons/m<sup>2</sup>sec

$\sigma_a$  = absorption cross-section =  $4 \times 10^{-16}$  m<sup>2</sup> [10]

$\sigma_s$  = stimulated emission cross-section =  $1.5 \times 10^{-16}$  m<sup>2</sup> [8]

$\alpha$  = quantum yield of intersystem crossing = 0.006 [9]

\* Both intensities ( $I_g$  and  $I_r$ ) are in photons per unit area per unit time

Figure 14 compares the number of molecules in the triplet state to the number of molecules in the singlet state during red beam illumination. According to Figure 14, the red probe beam starts to deplete the triplet state population at an intensity of  $10^{19}$  photons/m<sup>2</sup>sec. At this intensity, the theory curve shows only a slight change in the singlet state population. Figure 15 describes the behavior of molecules in the singlet state versus red beam intensity on an expanded scale. The population of the singlet state starts to increase at a red beam intensity of  $10^{19}$  photons/m<sup>2</sup>sec. This indicates that the molecules leaving the triplet state populate the singlet state, which results in fluorescence increase. The actual probe beam intensity ( $I_r$ ) was  $6.9 \times 10^{21}$  photons/m<sup>2</sup>sec, which is to the right of the maximum in Figure 15. The computed theoretical increase of fluorescence due to red light illumination is 1.29 %. This number was obtained by solving equation 15 and comparing the numbers of molecules in the singlet state for a red beam intensity of  $10^{18}$  photons/m<sup>2</sup>sec and  $6.9 \times 10^{21}$  photons/m<sup>2</sup>sec (actual intensity) as shown in Figure 15. The computed fluorescence increase is an upper limit value since we calculated the beam spot sizes, which illuminated the fluorescence dye with the following equation:

$$w = \frac{\lambda f / \pi w_0}{[1 + (\lambda f / \pi w_0^2)^2]^{1/2}} \quad \text{Eq.17}$$

where  $w$  is the calculated spot radius at the focus,  $w_0$  stands for the initial spot radius,  $f$  is the focal length, and  $\lambda$  stands for the wavelength of the focused light. In general, the actual spot diameter is larger than the calculated diameter from theory because of optical aberration, here, astigmatism causes a distortion of the spot size. Hence, the computed intensities are overestimated.

Another uncertainty in our theoretical calculation is the used value of the stimulated emission cross-section of the triplet state ( $\sigma_t$ ). We assumed that  $\sigma_t$  equals the stimulated emission cross-section ( $\sigma_s$ ). This assumption suggests that the obtained theoretical value is an upper limit.  $\sigma_s$  is likely to be greater than  $\sigma_t$  because the red beam overlaps with fluorescence emission (from the singlet state) more than with phosphorescence emission (from the triplet state).

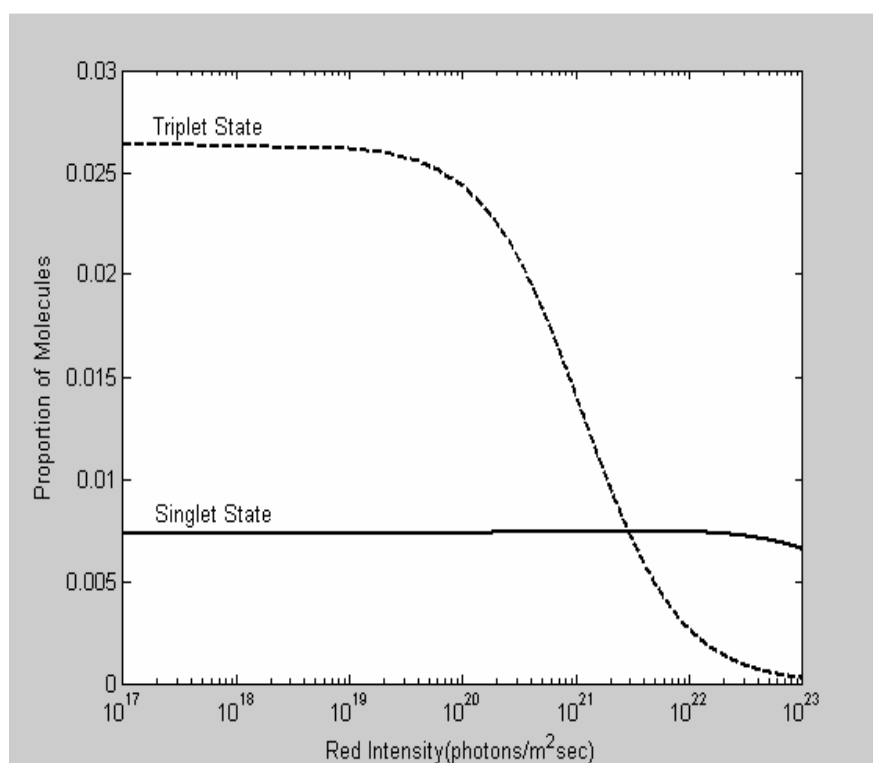


Figure 14: Number of molecules in the triplet and singlet state versus red beam intensity.

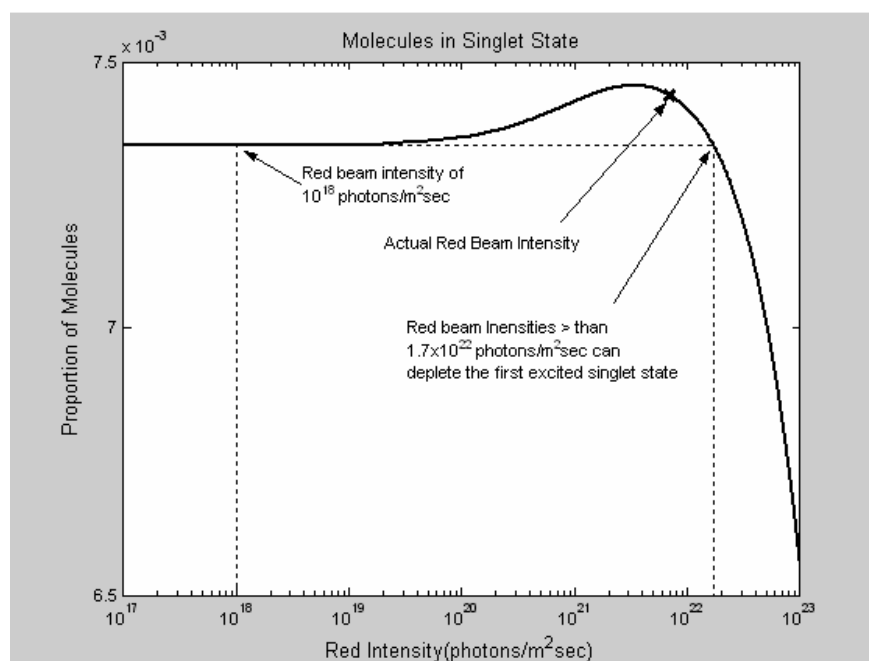


Figure 15: Number of molecules in singlet state versus read beam intensity

#### 4. Discussion

The experiments show stimulated emission of the triplet state is due to red light illumination. In order to obtain fluorescence depletion from the singlet state, we have to increase the intensity of the red probe beam. Quantitatively, we are able to deplete the singlet state during red light illumination if the red probe beam exceeds an intensity of  $1.7 \times 10^{22}$  photons/m<sup>2</sup>sec. The intensity of the red probe beam was measured to be  $6.9 \times 10^{21}$  photons/m<sup>2</sup>sec. If the red beam intensity is amplified by a factor of four, the singlet state could be depleted according to theory, because the number of molecules in the triplet state almost vanishes.

In addition to evanescent waves generated by total internal reflection (TIR), one could also use surface plasmon waves to excite the fluorophore. If a TIR interface is coated with a suitable conducting material, such as gold, the plane-polarized component of the evanescent wave may penetrate the metal layer and excite electromagnetic surface plasmon waves. These surface plasmons can enhance the initial intensity of the electromagnetic wave. It is theoretically possible, as outlined in the appendix (8.1), to obtain a red beam amplification of a factor of 4.7. Hence, surface plasmons can be used to sufficiently amplify the red probe beam intensity to decrease the singlet state population and cause stimulated photon emission. Moreover, if surface plasmons are

localized to island structures it could be used for resolution improvement and enhanced imaging.

Amplified surface plasmons can also improve the resolution limit in optical microscopy. This is significant for the study of biomolecular motion. J. Seidel [11] successfully demonstrated the amplification of surface plasmons by stimulated emission at the interface between a flat continuous silver film and a liquid containing organic dye molecules. He amplified surface plasmons through a pump beam, which excited plasmons at the metal's surface (at a fixed angle  $\theta_{spr}$ , set to the reflectance minimum of the pump light), and forced the dye molecule to emit its photons into the plasmon field by using a probe beam. This amplification can be detected by decreasing fluorescence signal when the probe beam is turned on, indicating fluorescence depletion by stimulated emission.

## 5 Conclusion

Intuitively, we expected to see fluorescence depletion from the singlet state in this experiment. Instead, we measured an increase in fluorescence. Careful analysis of the rate equations predicts that the signal increase we saw is due to stimulated emission from triplet state caused by the red pump beam. In a series of three follow-up experiments, we successfully confirmed that the measured increase of photon emission from the singlet state is due to triplet state depletion caused by the red probe beam. The theoretical fluorescence increase was determined to be 1.29 %. In our final experiment, we measured a fluorescence increase due to red light illumination of  $0.021 \pm 0.011$  %.

In order to observe stimulated emission from the first excited state the red probe beam intensity has to be increased. Surface plasmons could amplify the probe beam intensity by a factor of 4.7, which would be sufficient to see stimulated emission.

## 6 Acknowledgments

I would like to express my gratitude to the following people for their support and assistance with this senior project:

Dr. James L. Thomas, my research advisor for this great opportunity, and his enthusiastic guidance and help throughout the project.

Andy Maloney for his help in designing and machining parts.

The Undergraduate Committee for giving me the opportunity to present my Senior Thesis.

## 7 References

1. Sanong Ekgasit, Chuchaat Thammacharoen, Fang Yu, and Wolfgang Knoll, *Evanescence Field in Surface Plasmon Resonance and Surface Plasmon Field-Enhanced Fluorescence Spectroscopy*, Anal. Chem. 76. 2210-2219 (2004)
2. Thomas A. Klar, Egbert Engel, and Stefan W. Hell, *Breaking Abbe's diffraction resolution limit in fluorescence microscopy with stimulated emission depletion beams of various shapes*, Phys. Rev. E. 64, 066613 (2001)
3. J. Seidel, S. Grafstrom, and L. Eng, *Stimulated emission of Surface Plasmons at the Interface between a Silver Film and an Optically Pumped Dye Solution*, Phys. Rev. Lett. 94.177401 (2005)
4. David J. Griffiths, *Introduction to Electrodynamics*, Prentice Hall, 3<sup>rd</sup> ed., 1999. 576pp.
5. Lakowicz, *Principles of Fluorescence Spectroscopy*, Kluwer: New York. 1999. 698 pp.
6. J.Paul Robinson, *Lecture 3: Light and Fluorescence*, Purdue University, 2002  
[http://www.cyto.purdue.edu/flowcyt/educate/jpr/lecture003\\_files/frame.htm](http://www.cyto.purdue.edu/flowcyt/educate/jpr/lecture003_files/frame.htm)
7. R. Menzel, E. Thiel, *Intersystem crossing rate constants of rhodamine dyes: influence of the amino-group substitution*, Chem. Phys. Lett., 291 (1998) 237-243
8. M. Yamashita, A. Kuniyasu, and H. Kashiwagi, *Intersystem crossing rates and saturation parameters in the triplet state for rhodamine, fluorescein, and acridine dyes*, J. Chem. Phys., 66 (1977) 986-988
9. V.E. Korobov, V.V. Shubin, and A.K. Chibisov, *Triplet state of rhodamine dyes and its role in production of intermediates*, Chem. Phys. Lett., 45 (1977) 498-501
10. Oregon Medical Laser Center (OMLC) , *Rhodamine B*,  
<http://omlc.ogi.edu/spectra/PhotochemCAD/html/rhodamineB.html>

11. Stefan W. Hell and Jan Wichmann, *Breaking the diffraction resolution limit by stimulated emission: stimulated-emission-depletion fluorescence microscopy*, Opt. Lett., Vol.19, No.11, 1994
12. Luxpop, *Index of refraction values and photonics calculations*, <http://www.luxpop.com/>
13. Invitrogen, *Comparison of the fluorescence spectra of the Alexa Fluor 647 and Cy5 dyes*, <http://probes.invitrogen.com/handbook/figures/1749.html>
14. Raether, *Surface Plasmons on Smooth and Rough Surfaces and on Gratings*, Springer Verlag, 1988, 136pp
15. Verdeyen, *Laser Electronics*, Prentice Hall, 3<sup>rd</sup> ed., 1981
16. J. Thomas, personal communication, 12/04/06

## 8 Appendix

### 8.1 Calculation of Surface Plasmon Resonance

At an interface between two transparent media of different refractive index (glass and water), light coming from the side of higher refractive index is partly reflected and partly refracted. Above a certain critical angle of incidence, no light is refracted across the interface, and total internal reflection is observed. While incident light is totally reflected the electromagnetic field component penetrates a short distance into a medium of a lower refractive index creating an exponentially attenuating evanescent wave (Figure 2). If the interface between the media is coated with a thin layer of metal (gold), and light is monochromatic and plane-polarized, the evanescent field wave may penetrate the metal layer and excite electromagnetic surface plasmons. A surface plasmon is a collective excitation of the electrons at the interface between a conductor and an insulator. When surface plasmons are present, the intensity of the reflected light from the TIR interface is reduced at a specific incident angle producing a sharp dip (called surface plasmon resonance) due to the resonance energy transfer between evanescent wave and surface plasmons. The resonance conditions are influenced by the material adsorbed onto the thin metal film.

In order to produce surface plasmons, the prism used for total internal reflection has to be coated with a conducting material. Gold does not adhere well on glass. In order to evaporate gold onto glass, a pure titanium film has to be evaporated first to improve adhesion of the gold film.

Calculation for surface plasmon resonance (SPR), thin film reflectivity, transmission and absorption can be used to generate SPR curves for given values of titanium and gold layer thicknesses. We calculated surface plasmon resonance using a multilayer film model. This model was implemented as Matlab function (SPR\_4.m), which was written by me.

#### 1) Multilayer Configuration Glass-Titanium-Gold-Water

Known parameters :

- laser wavelength: 6330 (Å)
- titanium film thickness free parameter (0 - ∞Å)
- gold film thickness free parameter (0 - ∞Å)
- indices of refraction [12]:
  - Glass, left bound real index of refraction (BK7)  $n_1=1.51509$

- Water, right bound real index of refraction  $n_4=1.33$
- Titanium complex refraction index  $n_2=0.21-i*3.26$
- Gold complex refraction index  $n_3=0.21-i*3.26$

## 2) Calculation of complex angles of beam in all layers:

Glass-Titanium incident angle  $\theta_{-1}$

- Refracted angle  $\theta_{-2} = \sin^{-1}(n_1 * \sin(\theta_{-1})/n_2)$

Titanium-Gold incident angle  $\theta_{-2}$

- Refracted angle  $\theta_{-3} = \sin^{-1}(n_2 * \sin(\theta_{-2})/n_3)$

Gold-Water incident angle  $\theta_{-3}$

- Refracted angle  $\theta_{-4} = \sin^{-1}(n_3 * \sin(\theta_{-3})/n_4)$

## 3) Calculation of Stack Matrix (starting with the leftmost interface)

- 1) calculation of ( $\mathbf{H}_{12}$ ) interface transition matrix ( $n_1-n_2$ )  
with transmission and reflection coefficient for  $n_1-n_2$  interface
- 2) calculation of ( $\mathbf{L}_2$ ) layer propagation matrix ( $n_2$ )  
with corresponding phase factor
- 3) calculation of ( $\mathbf{H}_{23}$ ) interface transition matrix ( $n_2-n_3$ )  
with transmission and reflection coefficient for  $n_2-n_3$  interface
- 4) calculation of ( $\mathbf{L}_3$ ) layer propagation matrix ( $n_3$ )  
with corresponding phase factor
- 5) calculation of ( $\mathbf{H}_{34}$ ) interface transition matrix ( $n_3-n_4$ )  
with transmission and reflection coefficient for  $n_3-n_4$  interface
- 6) calculation of Stack Matrix

$$\mathbf{S} = (\mathbf{H}_{12}\mathbf{L}_2\mathbf{H}_{23}) \quad (1)$$

$$4) \text{ Calculation of reflection coefficient } (\rho) \quad \rho = S_{12}/S_{22} \quad (2)$$

$$\text{Calculation of Reflectance (R)} \quad R = |\rho|^2 \quad (3)$$

$$5) \text{ Calculation of transmission Coefficient } (\tau) \quad \tau = 1/ S_{22} \quad (4)$$

Calculation of Transmittance (T)

$$T = \frac{n_4 \cos \theta_4 |\tau|^2}{n_1 \cos \theta_1} \quad (5)$$

## 2) Calculation of the Evanescent Field E (outside gold surface)

Reference: M. V. Klein and T. E. Furtak, Optics,  
John Wiley & Sons 1986

### Known Parameters

- Laser wavelength  $\lambda = 6330 \text{ (\AA)}$
- Glass, left bound real index of refraction (BK7)  $n_1=1.51509$
- Water, right bound real index of refraction  $n_4=1.33$
- Incident angle (radians) =  $\theta_{\text{spr}}$  (Figure A1)
- Transmission coefficients  $\tau_1$  (air-glass) and  $\tau_2$  (refer equation 4)

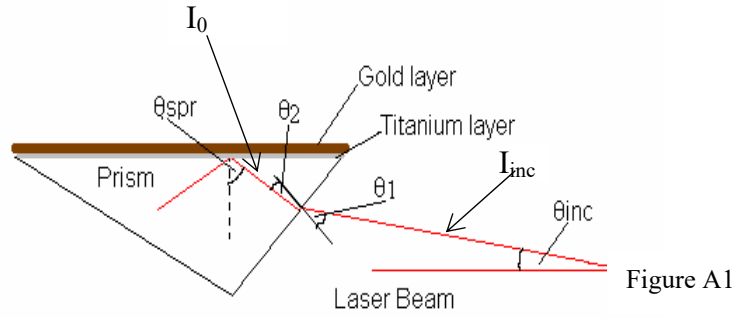


Figure A1

Complex notation for transmitted field ( $k_x$  and  $k_z$  are wave vectors):

$$E'(x,z,t) = E' e^{i(\omega t - \mathbf{k}' \cdot \mathbf{r})} = E' e^{i(\omega t - x k_x)} e^{-\gamma k_z z} \quad (6)$$

In the following computation the time  $t$  and position  $x$  of the electromagnetic wave are set to zero ( $t=0$  and  $x=0$ ) to obtain the expected exponential decay of the evanescent wave.  $E_0$  is the amplitude of the incident electric field on glass prism

$$E'(z) = E_0 \tau_1 \tau_2 e^{-\gamma k_z z} \quad (7)$$

$$\gamma = \sqrt{\frac{n_1 \sin \theta_{spr} - n_4^2}{n_1 \cos \theta_{spr}}} \quad (8)$$

$$k_z = 2 \frac{\pi n_1 \cos \theta_{spr}}{\lambda} \quad (9)$$

$$\tau_1 = 2 \frac{\sin \theta_2 \cos \theta_1}{\sin(\theta_1 + \theta_2) \cos(\theta_2 - \theta_1)} \quad (10)$$

$\tau_2 =$  refer equation (4)

Calculation of Enhancement Factor:

Ratio of  $|E'(z)|^2$  and incident electric field  $|E_0|^2$  gives the enhancement factor  $\mathbf{H}$  of the evanescent wave, which gives when multiplied by  $|E_0|^2$  the actual evanescent field intensity.

$$\mathbf{H} = \tau_1 \tau_2 e^{-\gamma k_z z} \quad (11)$$

This sequence of calculations was used to build the function intensity.m, which is able to generate the exponential decay of the electric field enhancement factor for known gold

film thickness, titanium thickness and given incident angle on total internal reflection (TIR) – interface.

Calculations involving intensity correction refer to Figure 1. Correction was needed to reduce free parameters, by calculating the transmittance (T) of the incident light for air-glass interface. R stands for reflectance in equations below

$$\rho = \frac{\tan(\theta_2 - \theta_{inc})}{\tan(\theta_2 + \theta_{inc})} \quad R = |\rho|^2 \quad T_{ag} = 1 - R$$

Final intensity correction:  $I_0 = I_{inc} / T_{ag}$

### 3) Created Theory Curves of Surface Plasmon Resonance

For the following theory curves, we assumed a gold film thickness of 300Å and titanium layer of 30 Å. Figure A2 shows reflectance of the glass-titanium interface (TIR interface, solid line) and reflectance of the glass-air interface (dashed line) versus incident angle. As shown in Figure A2, there is a dip in reflectance at 72.5°, which is above the critical angle (61°). The decreased reflectance in the metal-coated prism is caused by excitation of surface plasmons, which draw energy from the incident beam. In the absence of surface plasmons, the reflectivity of the red beam goes to 1 if the incident angle is greater than the critical angle.

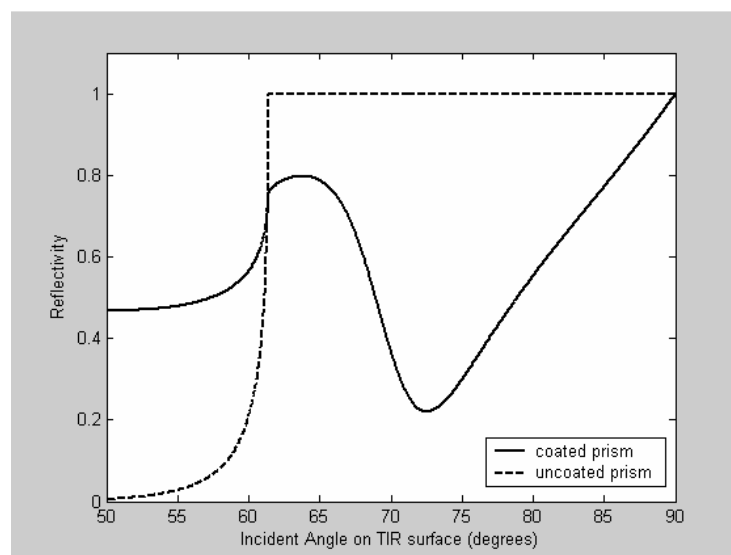


Figure A2: Reflectivity of incident red light on total internal reflection surface versus incident angle. Solid line represents surface plasmon curve for gold (300Å) and titanium (30 Å) coated prism. Dashed line shows reflectivity versus incident angle for uncoated prism.



```

%%%%%%%%%%%%%%%%%%%%%%%%%%%%%%%%%%%%%%%%%%%%%%%%%%%%%%%%%%%%%%%%%%%%%%%%
% Values
%%%%%%%%%%%%%%%%%%%%%%%%%%%%%%%%%%%%%%%%%%%%%%%%%%%%%%%%%%%%%%%%%%%%%%%%

lambda=6330;                % laser wavelength (angstroms)

l(2)=300;                   % metal 2 thickness in angstroms (gold)
l(3)=30;                    % metal 1 thickness in angstroms
(titanium)

n(1)=1.51509;              % left bound real index of refraction
(glass)
n(4)=1.33;                 % right bound real index of refraction
(water)
nmetall=2.1098;            % real refractive index of metal 1
kmetall=2.8794;           % imaginary refractive index of metal
n(2)=nmetall-kmetall*I;
nmetal2=0.21;             % real refractive index of metal 2
kmetal2=3.26;            % imaginary refractive index of metal 2
n(3)=nmetal2-kmetal2*I;

thetaideg=50;              % lower limit of calculation
thetaedeg=90;             % upper limit of calculation
thetai=thetaideg/180 *pi;
thetae=thetaedeg/180 *pi;

%%%%%%%%%%%%%%%%%%%%%%%%%%%%%%%%%%%%%%%%%%%%%%%%%%%%%%%%%%%%%%%%%%%%%%%%
% angles of incidence

samples=1001;
theta=thetai:(thetae-thetai)/(samples-1):thetae;
degtheta=theta*180/pi;
for k=1:samples
    s(k)=1;

%%%%%%%%%%%%%%%%%%%%%%%%%%%%%%%%%%%%%%%%%%%%%%%%%%%%%%%%%%%%%%%%%%%%%%%%
% calculation of stack matrix for each angle of incidence
%%%%%%%%%%%%%%%%%%%%%%%%%%%%%%%%%%%%%%%%%%%%%%%%%%%%%%%%%%%%%%%%%%%%%%%%

%%%%%%%%%%%%%%%%%%%%%%%%%%%%%%%%%%%%%%%%%%%%%%%%%%%%%%%%%%%%%%%%%%%%%%%%
% complex angles of the beam (thetal) in all layers

    thetal(1)= theta(k);
    thetal(2)= theta2(n(1),n(2),thetal(1));
    thetal(3)= theta2(n(2),n(3),thetal(2));
    thetal(4)= theta2(n(3),n(4),thetal(3));

%%%%%%%%%%%%%%%%%%%%%%%%%%%%%%%%%%%%%%%%%%%%%%%%%%%%%%%%%%%%%%%%%%%%%%%%
% STACK MATRIX (starting with leftmost interface)

    S = hmat(n(1),n(2),thetal(1));
    S = S*lmat(lambda,l(3),n(2),thetal(2)); % each sequential
propagation
    S = S*hmat(n(2),n(3),thetal(2)); % each sequential
interface
    S = S*lmat(lambda,l(2),n(3),thetal(3)); % each sequential
propagation
    S = S*hmat(n(3),n(4),thetal(3)); % each sequential
interface

    r(k)=(S(1,2)/S(2,2)); % Field Reflection

```

```

        rval(k)=r(k) * conj(r(k));           % Intensity reflection
end    %end for k=1:samples

%%%%%%%%%%%%%%%%%%%%%%%%%%%%%%%%%%%%%%%%%%%%%%%%%%%%%%%%%%%%%%%%%%%%%%%%
% Compute SPR angle
minimum=min(rval);
[mn,k]=min(rval);
for j=1:samples
    if degtheta(j)==minimum
spr_4=degtheta(j)
end
end

figure(2);
plot(degtheta,rval,'r');
title('SPR Curve Gold=, Titanium=');
xlabel('Incident Angle on TIR surface (degrees)')
ylabel('Reflectivity')

```

#### Additional functions needed:

```

function i=intensity(n1, n2, thet, lambda, ti)
% this function computes the intensity caused
% by the electric field ratio of E0 and E-evaescent
% with complex index of refraction for glass (n1), water (n2)
% using light of wavelength lambda (angstrom),incident angle thetal
% and transmission coefficient t calculated through stack matrix
% FORMAT:    intensity(n1, n2, thetal, theta2, lambda)

```

```

gamma = sqrt(((n1^2)*sin(thet)-(n2)^2)/(n1*cos(thet)));
gammamag = sqrt(gamma*conj(gamma));
kz = (2*pi*n1*cos(thet))/(lambda*10^(-10));
theta = (pi/2)-thet;
theta0 = asin(sin(theta)*n1);           % incident angle on prism
tair = (2*cos(theta0))/(cos(theta)+n1*cos(theta0));
magt = ti*conj(ti);
tairmag= tair * conj(tair);
a = gammamag*kz;
epsilon = 8.85418781762*10^(-12);
c = 3*10^8;
x = 0:0.00000001:1*10^(-6);

```

```

figure(2);
plot( magt * tairmag * exp(-2*a*x),'k');
title('Enhancement vs. Distance from Gold Surface');
xlabel('Distance (µm)');
ylabel('Enhancement Factor');

```

```

function H=hmat(n1,n2,theta1)
% This function generates the Interface Matrix between
% Two thin films. Output is a 2 by 2 matrix.
% Uses rho and tau subroutines.
% FORMAT:    HMAT(n1,n2,theta1)
c=1/tau(n1,n2,theta1);
H=c*[1 (rho(n1,n2,theta1)); (rho(n1,n2,theta1)) 1];

```

```

function t2 = theta2(n1,n2,theta1)
% This is a Matlab function that evaluates
% the complex angle of refraction based
% on snell's law.
% format:  theta2(n1,n2,theta1)
t = asin( (n1*sin(theta1)/n2));
    if imag(t)<0  t=conj(t);
end %if
t2 = t;

function t=tau(n1,n2,theta1)
% This function is the transmittance between two layers
% as determined by Maxwell's equations for Pi polarization
% FORMAT:  tau(n1,n2,theta1)
b= (n1/n2)^2 * (n2*cos(theta2(n1,n2,theta1)))/(n1*cos(theta1));
t= 2*(n1/n2)/(1+b);

function r=rho(n1,n2,theta1)
% This function is the reflectance between two layers as determined
% by Maxwell's equations for Pi polarization
% FORMAT:  rho(n1,n2,theta1)
i=sqrt(-1);
b= (n1/n2)^2 * (n2*cos(theta2(n1,n2,theta1)))/(n1*cos(theta1));
r=(1-b)/(1+b);

function L=lmat(lambda,l,n,theta)
% This function Generates the Layer Propagation Matrix
% Output is a 2 by 2 matrix
% FORMAT:  lmat(lambda,l,n,theta)
I=sqrt(-1);
c= (beta(lambda,l,n,theta));
L = [exp(-I*c) 0; 0 exp(I*c)];

function b=beta(lambda, l, n, theta)
% this function computes the phase differential caused
% by moving through a layer of thickness l at angle theta
% with complex index of refraction n using light of
% wavelength lambda
% FORMAT:  beta(lambda, l, n, theta)
b= 2*pi*n*l*cos(theta)/lambda;

```

## 8.2 Estimated Magnitude of Fluorescence Depletion in the Absence of Triplet State Effects

$A_{\text{det}} = 1.77 \times 10^{-6} \text{ m}^2$  (effective area of detector)  
 $A_{\text{cal}}$  = illuminated spot area calculated from laser intensity, I  
 $R_{\text{exp}} = 5 \times 10^3 \text{ Hz}$  (estimated rate of stimulated emission)  
 $R_{\text{sp}} = 5 \times 10^8 \text{ Hz}$  (rate of spontaneous emission 2ns)  
 $\sigma = 4 \times 10^{-16} \text{ m}^2$  (absorption coefficient of Rhodamine B at 543nm)  
 $P = 500 \mu\text{W} = 4.7 \times 10^{15} \text{ eV/s}$  (power of red laser)  
 $\lambda = 632 \text{ nm}$  (red HeNe laser)  
t = time in seconds  
 $\gamma$  = photon  
hc = 1242 nm

Red beam intensity:

$$I = \frac{\gamma}{tA_{cal}} = \frac{R_{exp}}{\sigma} = 1.25 \times 10^{19} \frac{J}{sm^2} \quad (12)$$

Number of photons per second (X) in red HeNe laser beam:

$$X = \frac{\gamma}{s} = \frac{J}{s} \frac{\gamma}{J} = \frac{P\lambda}{hc} = 2.4 \times 10^{15} \frac{\gamma}{s} \quad (13)$$

Now we can solve for  $A_{cal}$ :

$$A_{cal} = \frac{I}{X} = 1.92 \times 10^{-4} m^2 \quad (14)$$

The estimated ratio between effective detector area and calculated area of the spot is:

$$\frac{A_{cal}}{A_{det}} = 108.5 \quad (15)$$

Since the effected area of the detector is 100 times smaller than the calculated area of the spot size, the expected rate of stimulated emission will be,  $R_{exp} = 5 \times 10^5$  Hz. Then the ratio of spontaneous emission to stimulated emission is 1000, and we expect to observe an actual fluorescence depletion of 1 part in 1000.

### 8.3 Tabulated Raw Data

#### 8.3.1 Experiment 1:

Table A1

Measurement # 2: Sensitivity of lock-in amplifier was set to 100  $\mu$ V

Data taken (s)	Lock-in reading (%)	Signal amplitude ( $\mu$ V)	Mean ( $\mu$ V)	Standard error of mean ( $\mu$ V)
0	45	45		
40	46	46		
80	49	49		
120	50	50		
160	50	50		
200	51	51		
			48.5	0.99

Table A2

Measurement # 3: Sensitivity of lock-in amplifier was set to 100  $\mu\text{V}$ 

Data taken (s)	Lock-in reading (%)	Signal amplitude ( $\mu\text{V}$ )	Mean ( $\mu\text{V}$ )	Standard error of mean ( $\mu\text{V}$ )
0	28	28		
40	27	27		
80	28	28		
120	28	28		
160	27	27		
200	27	27		
			27.5	0.22

## 8.3.2 Experiment 2:

Table A3

Measurement #1: Sensitivity of lock-in amplifier was set to 10  $\mu\text{V}$ 

Data taken (s)	Lock-in reading (%)	Signal amplitude ( $\mu\text{V}$ )	Mean ( $\mu\text{V}$ )	Standard error of mean ( $\mu\text{V}$ )
0	34	3.4		
15	35	3.5		
30	33	3.3		
45	35	3.5		
60	36	3.6		
75	34	3.4		
90	36	3.6		
105	34	3.4		
120	29	2.9		
135	32	3.2		
150	34	3.4		
			3.38	0.06

Table A4

Measurement # 2: Sensitivity of lock-in amplifier was set to 100  $\mu\text{V}$ 

Data taken (s)	Lock-in reading (%)	Signal amplitude ( $\mu\text{V}$ )	Mean ( $\mu\text{V}$ )	Standard error of mean ( $\mu\text{V}$ )
0	16	1.6		
15	15	1.5		
30	15	1.5		
45	15	1.5		
60	16	1.6		
			1.54	0.02

Table A5

Raw data for measured red beam “transmitted” intensity change on green beam illumination.

NF density	Data taken (s)	Lock-in reading (%)	Sensitivity of lock-in
0	0	22	100 $\mu$ V
	15	24	
	30	26	
	45	30	
	60	25	
0.2	0	55	25 $\mu$ V
	15	59	
	30	58	
	45	65	
	60	45	
0.4	0	38	25 $\mu$ V
	15	35	
	30	35	
	45	39	
	60	35	
0.6	0	26	25 $\mu$ V
	15	26	
	30	27	
	45	30	
	60	29	
0.8	0	45	10 $\mu$ V
	15	40	
	30	43	
	45	41	
	60	45	
1.0	0	32	10 $\mu$ V
	15	35	
	30	35	
	45	34	
	60	35	
1.3	0	26	10 $\mu$ V
	15	26	
	30	27	
	45	27	
	60	26	
1.4	0	22	10 $\mu$ V
	15	22	
	30	22	
	45	22	
	60	22	
1.5	0	20	10 $\mu$ V
	15	20	

	30	21	
	45	21	
	60	20	
1.6	0	20	10 $\mu\text{V}$
	15	19	
	30	19	
	45	20	
	60	20	
2.0	0	16	10 $\mu\text{V}$
	15	17	
	30	16	
	45	16	
	60	17	
2.3	0	15	10 $\mu\text{V}$
	15	16	
	30	15	
	45	16	
	60	16	

Table A6

Column 2 calculated:  $10^{-\text{ND}}$ Column 3: subtracted 1.54  $\mu\text{V}$  (Table 2, measurement 2) from original signal (Table A5)

NF density	Intensity reduction	Signal ( $\mu\text{V}$ )	Standard Error
0	1	23.46	1.41
0.2	0.63096	12.56	0.82
0.4	0.39811	7.56	0.22
0.6	0.25119	5.36	0.2
0.8	0.15849	2.74	0.1
1.0	0.1	1.88	0.06
1.3	0.05012	1.1	0.02
1.4	0.03981	0.66	0
1.5	0.03162	0.5	0.02
1.6	0.02512	0.42	0.02
2.0	0.01	0.1	0.02
2.3	0.00501	0.02	0.02

## 8.3.3 Experiment 3

Table A7

Measurement #1: Sensitivity of lock-in amplifier was set to 250  $\mu\text{V}$ 

Data taken (s)	Lock-in reading (%)	Signal amplitude ( $\mu\text{V}$ )	Mean ( $\mu\text{V}$ )	Standard error of mean ( $\mu\text{V}$ )
0	-30	-75		
5	-35	-87.5		
10	0	0		

15	20	50		
20	20	50		
25	60	150		
30	40	100		
35	30	75		
40	20	50		
45	55	137.5		
50	60	150		
55	20	50		
60	10	25		
65	40	100		
70	30	75		
75	20	50		
80	40	100		
85	50	125		
90	60	150		
95	30	75		
100	0	0		
105	-10	-25		
110	10	25		
115	0	0		
120	-30	-75		
125	-20	-50		
130	-20	-50		
135	-15	-37.5		
140	-50	-125		
145	-50	-125		
150	-40	-100		
155	-40	-100		
160	-20	-50		
165	0	0		
170	-10	-25		
175	-40	-100		
180	-35	-87.5		
185	-25	-62.5		
190	-20	-50		
195	-20	-50		
200	-40	-100		
205	-20	-50		
210	-20	-50		
215	-40	-100		
220	-20	-50		
225	-20	-50		
230	-30	-75		
235	-40	-100		
240	10	25		
245	-10	-25		

250	-5	-12.5		
255	-5	-12.5		
260	60	150		
265	25	62.5		
270	40	100		
275	50	125		
280	60	150		
285	50	125		
290	70	175		
295	80	200		
300	70	175		
305	70	175		
310	70	175		
315	60	150		
320	30	75		
325	50	125		
330	20	50		
335	-10	-25		
340	20	50		
345	0	0		
350	20	50		
355	40	100		
360	40	100		
365	70	175		
370	60	150		
375	50	125		
380	95	237.5		
385	90	225		
390	70	175		
395	40	100		
400	40	100		
405	50	125		
410	60	150		
415	60	150		
420	10	25		
425	40	100		
430	40	100		
435	5	12.5		
440	-10	-25		
445	0	0		
450	0	0		
455	0	0		
460	10	25		
465	10	25		
470	70	175		
475	60	150		
480	60	150		

485	40	100		
490	40	100		
			46.5	22.65

## 8.4 Appended Figures

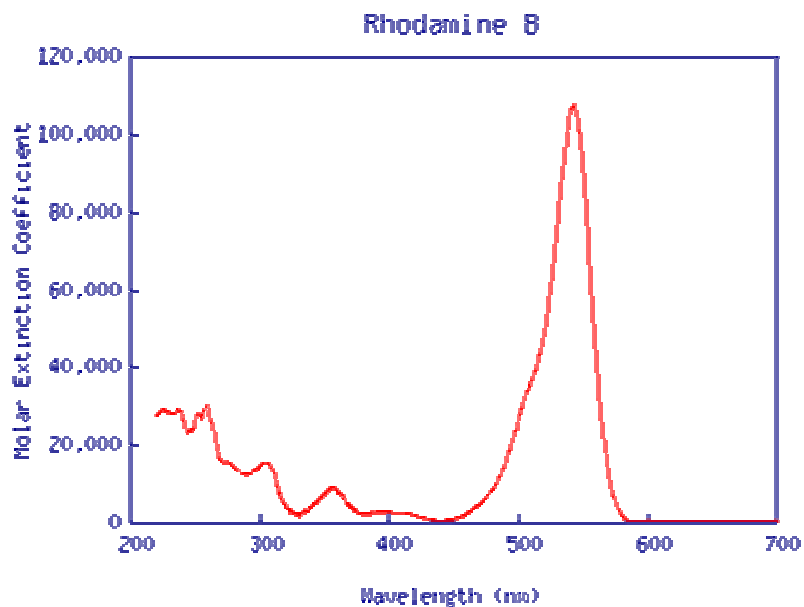


Figure A4: Absorption spectrum RhB [10].

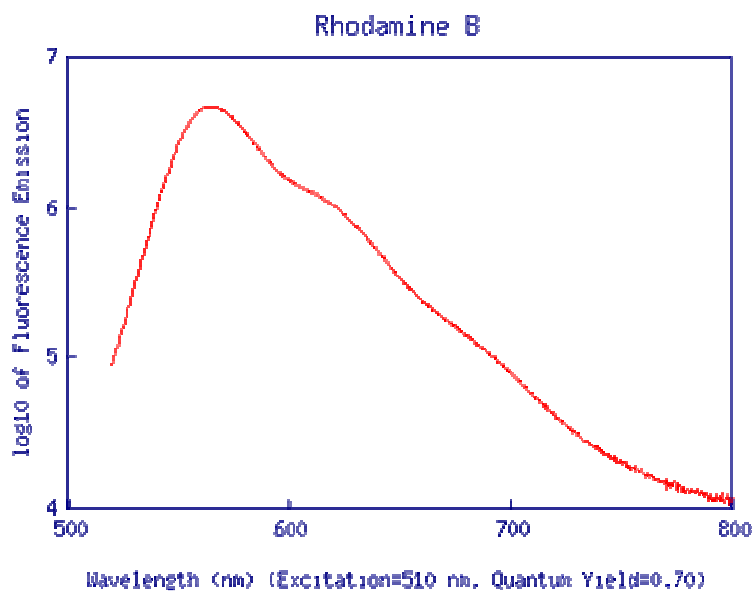


Figure A5: Emission spectrum RhB [10].

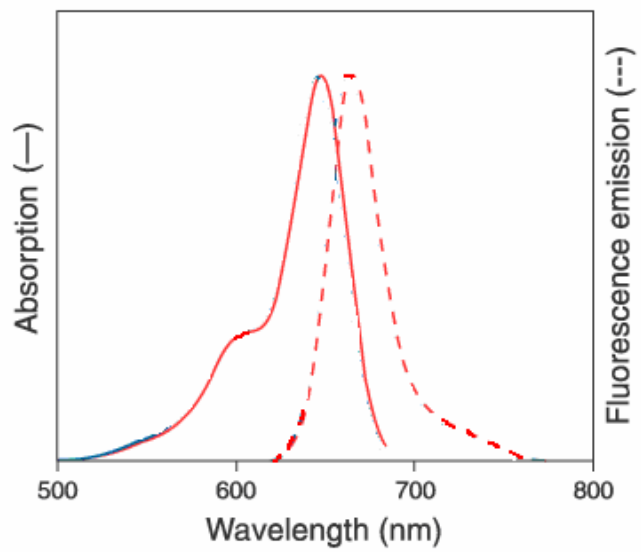


Figure A6: Absorption (solid line) and emission (dashed line) spectrum of Cy5 [13].